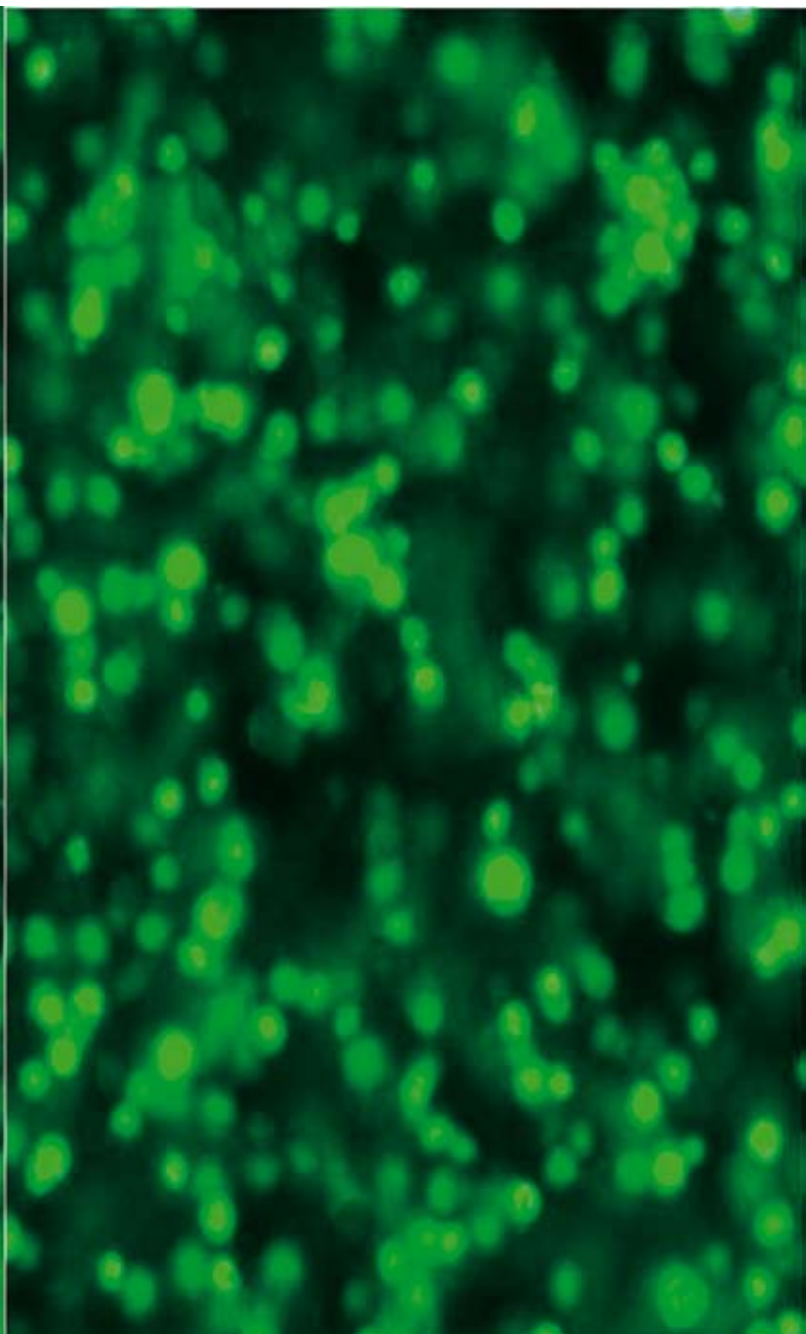
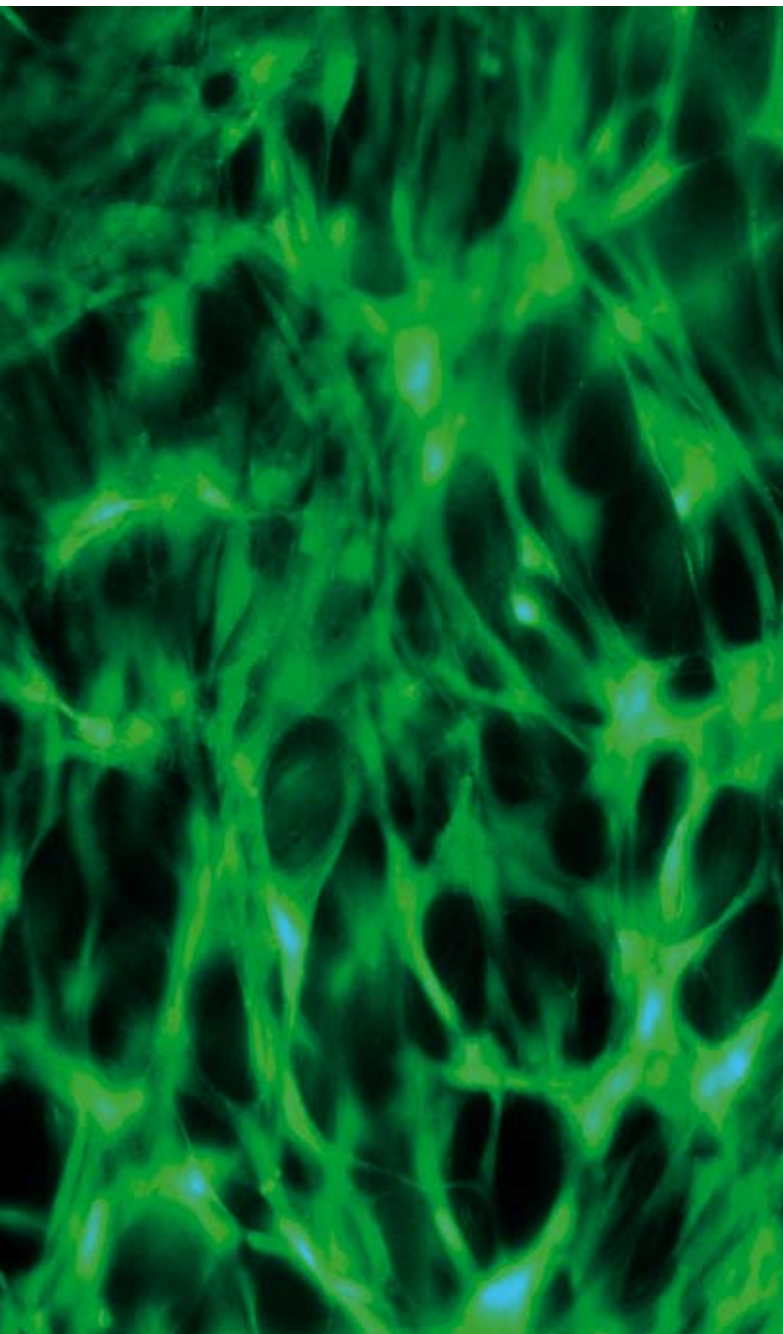


Soft Matter

www.softmatter.org

Volume 5 | Number 8 | 21 April 2009 | Pages 1541–1744



ISSN 1744-683X

RSC Publishing

PAPER

Jason A. Burdick *et al.*
Sequential crosslinking to control
cellular spreading in 3-dimensional
hydrogels

PAPER

Maura McEwan and David Green
Rheological impacts of particle softness
on wetted polymer-grafted silica
nanoparticles in polymer melts

Sequential crosslinking to control cellular spreading in 3-dimensional hydrogels

Sudhir Khetan, Joshua S. Katz and Jason A. Burdick*

Received 14th November 2008, Accepted 22nd December 2008

First published as an Advance Article on the web 11th February 2009

DOI: 10.1039/b820385g

With advanced understanding of how manipulations in material chemistry and structure influence cellular interactions, material control over cellular behavior (*e.g.*, spreading) is becoming increasingly possible. In this example, we developed a novel process that utilizes different crosslinking mechanisms to provide gel environments that are either permissive or inhibitory to cellular spreading. To accomplish this, a multi-acrylated macromer (*i.e.*, acrylated hyaluronic acid) was first crosslinked with an addition reaction using a matrix metalloprotease (MMP) cleavable peptide containing thiol groups. When an adhesive peptide was also coupled to the network, this environment permitted the spreading of encapsulated human mesenchymal stem cells (hMSCs), whereas control systems did not. If all acrylates were not consumed during the initial crosslinking step, a photoinitiated radical polymerization could be used to crosslink the remaining acrylates and inhibit cellular spreading with the production of covalent barriers. Variations in the ratio of the two crosslink types in individual constructs controlled the degradation and mechanical properties of the hydrogels, as well as the degree of spreading of encapsulated cells. Cell spreading was further controlled spatially with the use of photomasks. Overall, this new technology is an exciting and potentially valuable tool, both to provide new insights into the relationships between gel structure and cell behavior, and for eventual tissue-engineering applications where spatial control over cells is desired.

Introduction

Cellular spreading is important in that it allows cells to interact with their environment, including receiving cues towards proliferation and even differentiation.¹ Until recently, the scaffolding component in tissue engineering has been employed as a relatively inert component to the approach, providing mainly structural support and potential adhesion interactions through decoration with peptides and proteins.^{2–5} However, it is now clear that the dynamic interplay that occurs between cells and the extracellular matrix (ECM) is also important in the design and functionality of new biomaterials for use as synthetic cellular environments. The ECM is a dynamic and biologically active matrix with critical structural and functional roles, and ECM remodeling is necessary for cell migration and tissue morphogenesis.

Cellular spreading, which varies *in vivo* according to cell type and biochemical and mechanical properties of different tissues, may influence cellular functions such as stem cell differentiation.^{6–8} Past work indicates that hMSCs seeded onto substrates coated with adhesive elements such as fibronectin,⁹ collagen,¹⁰ and gelatin¹¹ differentiate depending on adhesion, morphology, and spreading. Curran *et al.* demonstrated that differences in morphology of hMSCs adhered to glass substrates with modified surface chemistries led to differences in differentiation.^{12,13} The importance of cell shape in terminal differentiation has also been

demonstrated for other progenitor cell types ranging from bone marrow stromal cells⁷ to human epidermal keratinocytes.¹⁴

Recent studies have incorporated ECM-mimetic features into hydrogels in a 3-dimensional (3-D) fashion to control encapsulated cellular behavior. For example, it has been shown that the viability and proliferation of hMSCs encapsulated in synthetic PEG-based hydrogel networks depends on the adhesiveness of the surrounding matrix.³ Beyond adhesion, Lutolf *et al.*¹⁵ demonstrated that spreading and random migration of fibroblasts encapsulated in PEG-based hydrogels was possible when both cell-adhesivity and MMP-degradability were incorporated into the networks. They have since explored this system for cardiac tissue-engineering applications,¹⁶ showing that multipotent cardioprogenitors encapsulated in the networks differentiated along the cardiac lineage when the stiffness of the scaffold mimicked that of native cardiac tissue. In a similar manner, Kim *et al.*¹⁷ incorporated cell-adhesivity and proteolytic degradability into hyaluronic acid (HA)-based scaffolds and demonstrated spreading of encapsulated hMSCs, something that was not possible in gels lacking either bioactive feature. Others have also utilized hydrogels containing these cues for tissue-engineering approaches.^{18–20}

Despite these approaches, very few studies have investigated the spatial control that may be possible in these environments. In one example, investigators micropatterned cell-adhesive oligopeptides into precisely defined channels and demonstrated guided neurite outgrowth.^{21,22} However, the spatial control of encapsulated cell behavior using a cytocompatible process has not yet been achieved; the described 3-D studies all employed a single mode of crosslinking (*e.g.*, addition reactions between

Department of Bioengineering, University of Pennsylvania, 240 Skirkanich Hall, 210 South 33rd Street, Philadelphia, PA 19104, USA. E-mail: burdick2@seas.upenn.edu

peptide thiol groups and vinyl double bonds) homogeneously throughout the matrix volume, whereas the spatially controlled hydrogels did not use processes that were compatible with cells. A technique that affords such spatial control would be useful in numerous applications, from fundamental investigations of the influence of gel structure on cellular behavior to tools for advanced tissue-engineering applications.

In this work, we present a novel material-based process that utilizes multiple modes of crosslinking in a sequential manner to spatially control the behavior of cells encapsulated within 3-D hydrogels (this process is shown schematically in Fig. 1). During the primary step, hydrogels that contain both adhesive sites and MMP-cleavable dithiol crosslinkers are formed from multi-acrylate macromers (*i.e.*, acrylated hyaluronic acid) *via* an addition mechanism, leaving a network that is “permissive” to remodeling and cellular spreading. Importantly, only a portion of the total number of acrylate groups is consumed during this first step, which occurs in the presence of a photoinitiator (at this point, non-reactive). During the secondary step, the gels are exposed to light to initiate radical polymerization of all the remaining acrylates, creating a network that is “inhibitory” to cell spreading based on the covalent crosslinks formed through kinetic chains. The premise is that the covalent crosslinks block cellular remodeling and prevent cellular spreading in the hydrogels since the mesh sizes are significantly smaller than typical cell diameters.^{17,23} Since the second step is initiated by light, which can be spatially controlled, it is anticipated that this approach may be useful to spatially control cellular spreading within the hydrogels. This report describes the process and its utility in controlling stem cell behavior in 3-D hydrogel environments.

Experimental

AHA synthesis

Acrylated hyaluronic acid (AHA) was synthesized *via* a 3-step protocol. All ¹H NMR spectra were recorded on a Bruker Avance 360MHz spectrometer.

Synthesis of HEA-succinate (HEA-suc). Succinic anhydride (1.5 eq.) and 2-hydroxyethyl acrylate (1 eq.) were combined in a 500 mL three neck round bottomed flask. Following a purge of nitrogen, 200 mL of anhydrous dichloroethane was cannulated into a flask and the reaction was heated to 65 °C. 1-Methylimidazole was added as a catalyst (0.06 eq.). The reaction was allowed to proceed for 18 h at 65 °C. The product was purified by extractions with aqueous 0.1 M HCl and 1 M NaCl and the

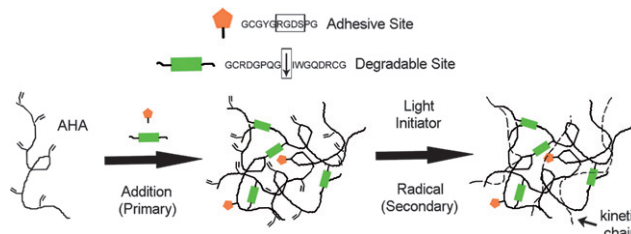


Fig. 1 Schematic of sequential crosslinking of AHA using a primary addition reaction and a secondary radical polymerization.

organic layer was dried with MgSO₄. To avoid polymerization, a small amount of hydroquinone was added prior to drying. NMR (CDCl₃): δ (ppm) 2.70, 4H, m; 4.37, 4H, m; 5.87, 1H, dd; 6.14, 1H, dd; 6.44, 1H, dd.

Synthesis of the tetrabutylammonium salt of HA (HA-TBA).

Sodium hyaluronate (1 eq.) was dissolved in 200 mL DI H₂O to give a ~1 wt% solution. To this solution, the highly acidic ion exchange resin, Dowex-100 (3 eq., by mass), was added, and the slurry was stirred for 8 h, at which point the solution was filtered to remove the resin. The acidic solution was neutralized with 0.2 M tetrabutylammonium hydroxide (TBA-OH) to pH 7.02–7.05, forming a quaternary ammonium salt of hyaluronate and the tetrabutylammonium group (HA-TBA). The solution was frozen and lyophilized to yield the dry product. NMR (D₂O): δ (ppm) 4.2–4.6, 2H; 3.15–3.9, 10H; 3.1, 8H, dd; 1.9, 3H; 1.5, 8H; 0.82, 12H.

Coupling of HEA-suc and HA-TBA. HA-TBA (1 eq., repeat unit) and dimethylaminopyridine (DMAP, 0.075 eq.) were combined in an oven-dried 3-neck round-bottomed flask under nitrogen. The amount of DMAP and HEA-suc added relative to HA-TBA was varied to achieve different percentage acrylate functionalities. Anhydrous DMSO was cannulated into the sealed flask to give a roughly 1 wt% HA-TBA solution. The flask was heated to 45 °C, and following complete dissolution of the contents, di-*tert*-butyldicarbonate (1.5 eq.) was injected into the flask and the reaction was allowed to proceed for 18 h. The solution was then diluted 1 : 1 with DI H₂O, dialyzed extensively against DI H₂O, frozen, and lyophilized to yield the dry product.

The final structure and ¹H NMR spectrum of AHA are shown in Fig. 2. NMR (D₂O): δ (ppm) 6.4, 0.4H, d; 6.15, 0.4H, dd; 5.9, 0.4H, d; 4.2–4.6, 2H; 3.15–4.0, 10H; 2.7, 1.2H, broad; 1.9, 3H, s.

Cells

Human mesenchymal stem cells (hMSCs) were obtained from Lonza Corporation (Wakersville, MD, USA). For encapsulation studies, hMSCs were expanded in growth media (α-MEM, 10% FBS, 1% L-glutamine & penicillin streptomycin) and encapsulated at low passage numbers (between 2 and 4) in AHA hydrogels at a density of 5 × 10⁶ cells per mL. The constructs

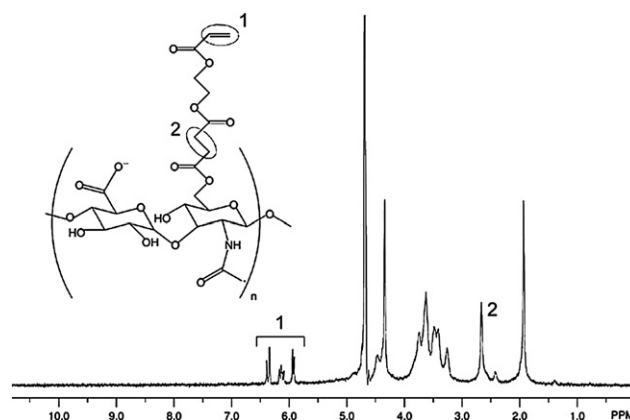


Fig. 2 ¹H NMR Spectrum (D₂O) of acrylated hyaluronic acid (AHA).

were maintained in 1.5 mL of growth media in a 24-well plate and refreshed every 3 days until the end of day 5, at which point live/dead analysis was performed.

Peptides

The cell adhesive oligopeptide GCGYGRGDSPPG (M_w : 1025.1 Da) and MMP-degradable oligopeptide GCRDGPQG↓IWGQDRCG (M_w : 1754.0 Da), both with >95% purity (per manufacturer HPLC analysis), were obtained from GenScript Corporation (Piscataway, NJ, USA) for all studies.

Crosslinking

AHA was dissolved in a triethanolamine-buffered saline (TEOA buffer: 0.2 M TEOA, 0.3 M total osmolarity, pH 8.0) containing Irgacure2959 (Ciba) photoinitiator (final concentration of 0.05 wt%). I2959 was chosen due to its aqueous solubility and good cytocompatibility.²⁴ The cell adhesive peptide dissolved in TEOA buffer was added to the AHA solution at a final peptide concentration of 1 mM (corresponding to $\sim 1/20$ of available acrylate groups with 3 wt% AHA), and allowed to react for 1 h at 37 °C. Following re-suspension of cells in this solution, MMP peptide dissolved TEOA buffer was added to the pre-polymer solution corresponding to the desired percent acrylate consumption, and 50 μ L of this mixture was immediately pipetted into sterile molds (5 mm diameter, 2 mm height). The gels were allowed to react (primary crosslinking) for 15 min at room temperature inside the laminar flow hood. For sequential crosslinking studies, gels were then exposed to 10 mW cm⁻² 365 nm ultraviolet light (Omniscure S1000 UV Spot Cure System, Exfo Life Sciences Division, Mississauga, Ontario, Canada) for 4 minutes (secondary crosslinking). Gelation times were chosen based on earlier acellular experiments that measured the addition and radical polymerization durations (15 and 4 min, respectively) for which further reaction did not change the mechanical properties.

Hydrogel characterization

Acellular samples were fabricated as described above. Following crosslinking and swelling to equilibrium in PBS for 24 h, the Young's modulus of each hydrogel disk was determined by unconfined submersion compression testing on a dynamic mechanical analyzer (Q800 Series; TA Instruments, New Castle, DE, USA) with an oscillating plate compression clamp attachment. Briefly, the diameter of each swelled hydrogel disk (~ 5 mm) was determined using a digital caliper, and the sample was immersed in a PBS bath between unconfined parallel compression plates to prevent dehydration. An equilibrium preload force was applied by the descending plate, followed by application of a ramped strain of 10% min⁻¹ to 60%. The Young's modulus was then determined using the slope of the stress-strain curve at low strain (<25% strain). To obtain the volumetric swelling ratio (Q_v), equilibrium swelled constructs were patted dry to remove surface liquid and weighed (wet weight), lyophilized, and reweighed (dry weight). Q_v is reported as the ratio of the wet weight to dry weight, assuming a density of 1.23 g cm⁻³ for the AHA macromers.²⁵ For degradation studies, hydrogels that crosslinked completely (*i.e.*, 100% acrylate consumption)

through addition or radical polymerization were incubated in separate wells of a 24-well plate containing 1 mL PBS with 40 nM human MMP-1 (Sigma) on an orbital shaker at 37 °C. The solutions were refreshed every 24 h for 1 week, and the supernatant samples (frozen and stored at -20 °C after collection) were analyzed in triplicate *via* a modified uronic acid assay.²⁶ Briefly, 100 μ L of each sample was added to a concentrated solution of sulfuric acid and sodium tetraborate decahydrate (Sigma) and heated to 100 °C for 10 min. 100 μ L of 0.125% carbazole solution in ethanol was then added, and the samples were vortexed and heated to 100 °C for 15 min. The sample absorbances were then read at 530 nm and compared to a standard curve of known concentrations of HA (a range from 0.1 to 2.0 mg mL⁻¹). All studies were performed in triplicate unless otherwise noted.

Live/dead staining

Encapsulated cells were visualized for viability using a fluorescent live/dead staining kit (Molecular Probes) and imaging on an inverted microscope (Axiovert 200, Carl Zeiss Inc.) equipped with an epifluorescent lamp. For assessment of viability, three random images of each gel at 5 \times magnification were taken through both the live (FITC) and the dead (TRITC) filters. Cell viability was then assessed by counting the total number of live and dead cells in each image and calculating the ratio of live cells to total cells. For all cellular images, each construct was first viewed from the top to the bottom surface to ensure uniform cellular morphology throughout the construct volume and that images were obtained from the interior of the gel.

Cellular aspect ratio measurements

For cellular aspect ratio measurements, three random light microscopy images at 5 \times magnification were taken from each gel using an inverted microscope. To quantify cellular spreading, the maximum orthogonal length and width of each cell was measured using NIH ImageJ, and the aspect ratio calculated as the longer length divided by the shorter length. Each image produced ≥ 15 measurements from randomly selected cells, or $n \geq 45$ for each sample. The measured aspect ratios were then sorted into bins to form histograms of spreading for each formulation.

Statistical analysis

All values are reported as the mean \pm standard error of the mean. ANOVA in conjunction with Tukey's post hoc test was used to determine statistically significant differences between groups, with $p \leq 0.05$.

Results and discussion

Acellular hydrogel synthesis and characterization

AHA with 38% of hydroxy groups acrylate-modified was synthesized and the acrylation conversion was measured *via* ¹H NMR as described. The purified yield was $\sim 65\%$ based on moles of HA present in the HA-TBA reactant and AHA product. HA, a linear glycosaminoglycan made of alternating D-glucuronic

acid and *N*-acetyl-D-glucosamine, was used as the primary structural component due to its biocompatibility, hydrophilicity, importance *in vivo* including in the turnover of ECM following tissue injury, interactions with cells *via* surface receptors,^{27,28} and past use in tissue-engineering applications.^{29–33} Although HA is commonly modified with methacrylate groups, acrylate groups were used since they react much faster during the primary addition step,^{34,35} which allows for uniform cell suspensions. While HA was used in the current work, the sequential crosslinking technique may potentially be applied to other macromers functionalized with reactive groups that can undergo multiple modes of crosslinking, highlighting its versatility.

AHA was crosslinked into 3 wt% hydrogels either with a photoinitiated polymerization alone, with an addition polymerization alone, or sequentially using both (in order) an addition and radical polymerization. For the addition polymerizations, theoretically 50, 75, or 100% of the acrylates were consumed. ¹H NMR was used to confirm a decrease in the acrylate peaks upon addition crosslinking and elimination of the acrylate peaks with photopolymerization. Additionally, peak reduction corresponded to the theoretical amount of acrylate consumption (data not shown).

Both the mechanics and the swelling of the hydrogels were dependent on the type of crosslinking (and for sequentially crosslinked gels, the ratio of addition to radical crosslinking) that was used (Fig. 3A and 3B). Hydrogels crosslinked only through radical polymerization exhibited a ~2–4-fold higher compressive modulus (18.62 ± 1.96 kPa) and swelled significantly less ($Q_V = 27.75 \pm 1.20$) than either addition alone (*e.g.*, modulus = 4.60 ± 0.71 kPa, $Q_V = 45.42 \pm 1.70$ for 50% formulation) or

sequentially crosslinked (*e.g.*, modulus = 9.45 ± 2.90 kPa, $Q_V = 38.26 \pm 2.68$ for 50% + photo formulation) hydrogels. 100% addition samples polymerized too quickly to obtain uniform samples suitable for mechanical testing. The kinetic chains in the radically crosslinked only hydrogels concentrate the acrylate side chains and create a more dense network than those that are reacted with a dithiol oligopeptide crosslinker molecule, as in the addition reaction. This could explain the higher modulus and decreased swelling in radical only hydrogels. Sequentially crosslinked hydrogels with identical peptide compositions but secondarily crosslinked through photopolymerization exhibited increased moduli and decreased swelling relative to their addition-only counterparts, indicative of the secondary radical polymerization. These changes were greater for the 50% case, since a higher percentage of acrylate groups was available for the radical crosslinking step.

AHA hydrogels synthesized completely (*i.e.*, 100% acrylate consumption) through the addition or radical crosslinking mechanisms also differed predictably in degradation kinetics when incubated in PBS containing 40 nM MMP-1 (Fig. 3C). Hydrogels crosslinked with MMP-degradable oligopeptides underwent complete degradation *via* the action of exogenous proteases by day 7, while radically crosslinked gels showed little mass loss (~10%, with kinetics that mimicked incubation in PBS alone) potentially from hydrolysis of ester linkages in the crosslinks or a soluble fraction after crosslinking. These results support the underlying premise that the covalent kinetic chains do not allow for proteolytic degradation, whereas the MMP cleavable crosslinks degrade rapidly in the presence of the enzyme. These trends also illustrate the potential tunability of the sequential crosslinking system, as both the concentration of MMP-degradable domains (*i.e.*, the degradation kinetics of the hydrogel in the presence of MMP) and bulk mechanical properties can be matched to the tissue-engineering application of interest.

Controlled encapsulated cell spreading in bulk polymerized gels

To determine if these results translate into cellular instructive hydrogels, hMSCs were suspended in the initial macromer solution and encapsulated using either the photoinitiated polymerization alone or the sequential crosslinking procedure.

The addition alone hydrogels with 100% acrylate consumption polymerized too quickly to obtain evenly distributed cells and were not further investigated. Control hydrogels (shown in Fig. 4) were produced that contained only the MMP-degradable peptide crosslinker, but no RGD peptide (–RGD, MMP); the RGD peptide, and alternate non-degradable dithiol crosslinker dithiothreitol (+RGD, DTT); and containing RGD peptide but crosslinked using a photoinitiated radical polymerization alone (+RGD, photo). As expected, hMSCs in these constructs remained rounded (Fig. 4a), with 100% of the cells exhibiting an aspect ratio (*i.e.*, the ratio of the longest to shortest dimension of encapsulated cells) between 1 and 2 (Fig. 4b). In contrast, when adhesivity and degradability were incorporated into single gels (+RGD, MMP), robust cell spreading was observed and found to be dependant of the relative amount of each crosslinking mode (Fig. 5). Cells encapsulated in “permissive” hydrogels synthesized only through addition crosslinking using

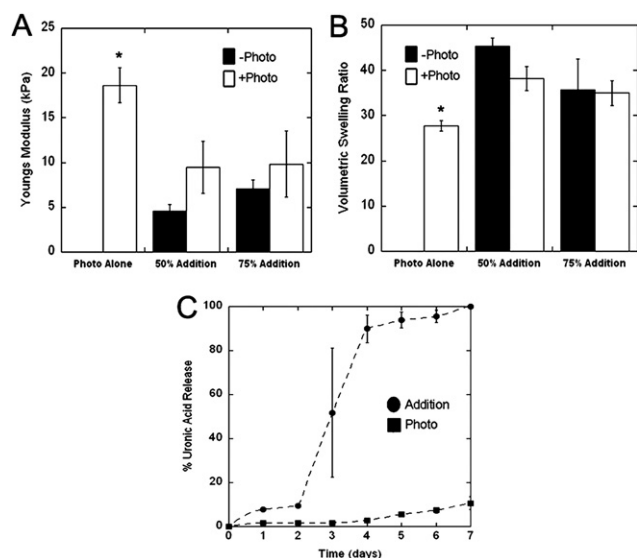


Fig. 3 Characterization of sequentially crosslinked AHA hydrogels. (A) Compressive modulus and (B) swelling ratio of photopolymerized and sequentially crosslinked AHA hydrogels. The sequential crosslinking was performed with a theoretical consumption of either 50% or 75% of acrylates on the AHA during the primary crosslinking. * denotes statistically significant difference from all other cross groups. (C) Degradation kinetics of AHA hydrogels crosslinked using only an addition or radical mechanism (100% theoretical consumption of acrylates in both cases) in the presence of 40 nM MMP-1.

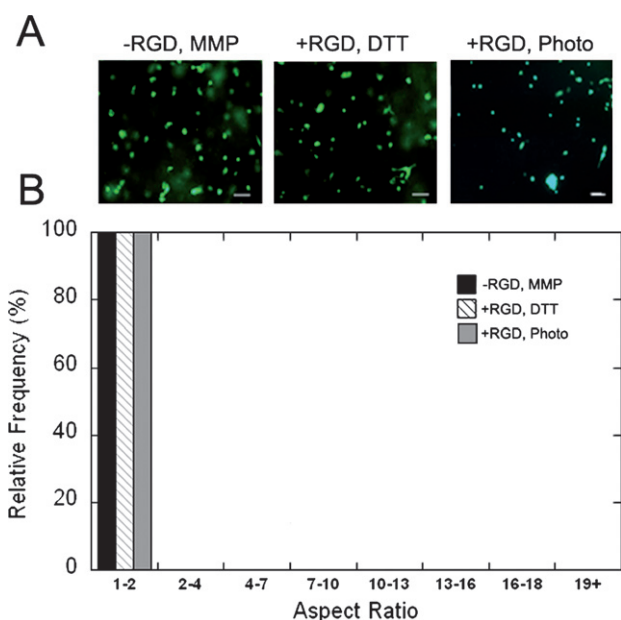


Fig. 4 hMSC encapsulation in control AHA hydrogels. (A) Images of encapsulated hMSCs in hydrogels formed using (respectively) MMP-degradable peptide crosslinker in the absence of RGD peptide, with the non-degradable dithiol crosslinker (DTT), and containing RGD peptide but crosslinked using radical polymerization alone. Scale bar represents 100 μm . (B) Histogram of the cellular aspect ratio (the ratio of the longest to shortest dimension of encapsulated cells) for these same groups. All cultures were run for 5 days. There were no statistically significant differences between these groups.

MMP-degradable peptides corresponding to 50% and 75% acrylate consumption exhibited relatively high degrees of spreading (*i.e.*, a distribution towards much higher aspect ratios in Fig. 5b). However, cells encapsulated in “inhibitory” hydrogels formed with the sequential crosslinking procedure were similar to the radical polymerization alone and remained rounded. This inhibition was more pronounced with a lower fraction of acrylates consumed during the addition step (50% *versus* 75%), potentially due to the greater amount of crosslinking during the secondary radical polymerization to inhibit spreading. As others have reported,^{16,18} these results indicate that both adhesion and degradation sites are necessary for cellular remodeling of synthetic hydrogels.

Cells in all conditions exhibited high viability (88–94%) as quantified from live/dead staining (dead stain overlaid on Fig. 4 and Fig. 5 live images), with no statistical differences between any of the hydrogel compositions (data not shown).

Spatially controlled encapsulated cell spreading

Although these results illustrate our ability to form gels that either permit or inhibit cell spreading, there are many instances where this would be beneficial to achieve with spatial control. As discussed, it is clear that cues such as spreading lead to changes in cell signaling and potentially differentiation; thus, spatial control over spreading could lead to control over cell lineage towards the development of advanced tissue-engineering approaches with differentiation down multiple cell lineages. In this sequential

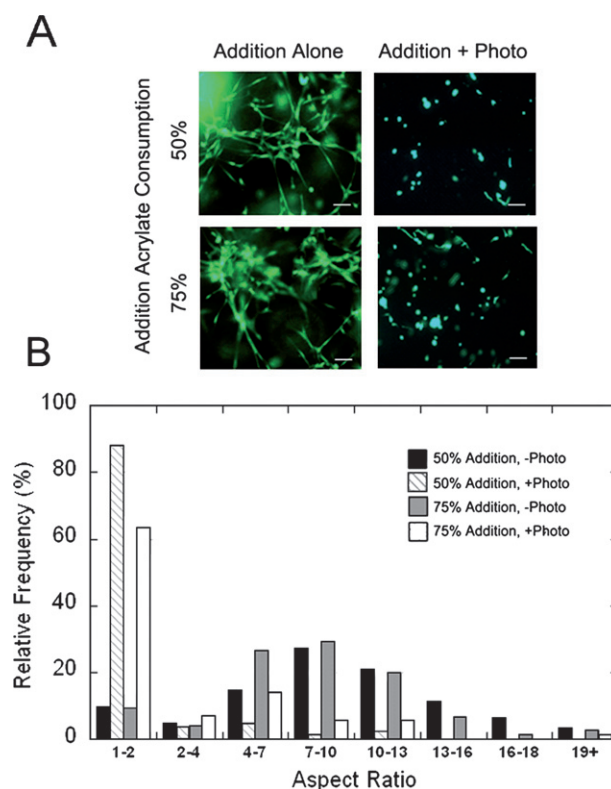


Fig. 5 hMSC encapsulation in sequentially crosslinked AHA hydrogels. (A) Images of encapsulated hMSCs in hydrogels formed by an addition polymerization alone or using the sequential polymerization procedure. The sequential crosslinking was performed with a theoretical consumption of either 50 or 75% of acrylates on the AHA during the primary crosslinking. Scale bar represents 100 μm . (B) Histogram of the cellular aspect ratio (the ratio of the longest to shortest dimension of encapsulated cells) for these same groups. All cultures were run for 5 days. There were statistically significant differences for the aspect ratios between the addition polymerization alone and the sequential polymerization for each formulation (*i.e.*, 50 or 75% acrylate consumption).

crosslinking approach, the creation of spatially controlled spreading of AHA hydrogels can be achieved by applying a photomask between the two crosslinking steps (Fig. 6A). As illustrated, regions of the hydrogel that are unmasked are exposed to light and undergo a secondary radical polymerization, while masked regions are not exposed to the light and only undergo the primary crosslinking.

To illustrate the feasibility of this approach, AHA hydrogels synthesized with 50% consumption during the primary crosslinking were exposed to light through a mask that blocked half of the sample in entirety. A live image of cells at the interface in this gel is shown in Fig. 6B and indicates spherical morphology with light exposure and spindle-like morphology in areas that were covered with the mask. The extent of outgrowth in these regions, both qualitatively from light microscopy and as quantified through aspect ratio measurements (Fig. 6C), were similar to the corresponding bulk gels assessed above. Although this is a simple example of the approach, more complex patterns could be achieved with different masks or through the use of lasers for the secondary polymerization.^{36,37}

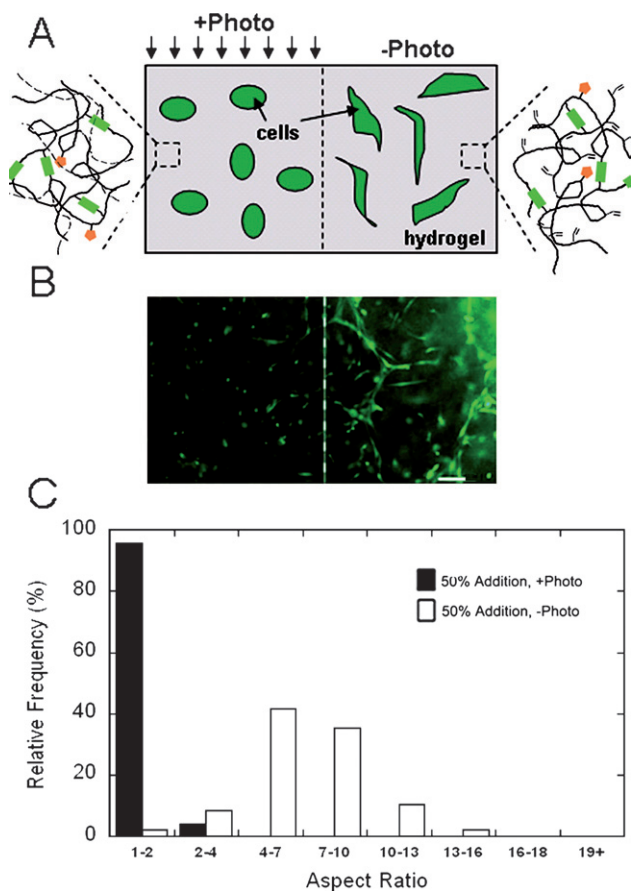


Fig. 6 Spatially patterned outgrowth of hMSCs. (A) Schematic of process to spatially control cell spreading in AHA hydrogels. (B) Calcein-stained hMSCs encapsulated in a sequentially crosslinked AHA hydrogel where one half of the construct was covered with a mask during light exposure. Scale bar represents 100 μm . (C) Histogram of cell spreading in regions exposed to light (addition + radical) or covered with a mask (addition only) during the secondary crosslinking. All cultures were run for 5 days. There was a statistically significant difference between aspect ratios in regions exposed to and masked from light.

Conclusions

The sequential polymerization described here is a robust, novel approach towards dictating the cellular behavior in 3-dimensions. While a single AHA weight percentage was used in the current study, the versatility of the sequential crosslinking technology arises from the ability to vary this and other design parameters (e.g., HA acrylation efficiency, macromer and peptide concentrations, encapsulated cell density) to tune the remodeling kinetics to different applications. For instance, differences in cellular morphology in patterned AHA hydrogels could be useful as a signaling mechanism for spatially controlled differentiation of encapsulated stem cells. Such an approach has potential in the regeneration of tissues with anisotropic properties (e.g., vasculature or nervous tissues) or where spatially controlled organization of cells is desired. In the current work, the cells were cultured in standard growth medium to illustrate the technique of controlled spreading, and no specific cell type or tissue was targeted. Collectively, this approach may become a valuable tool in biomaterials development and regenerative medicine.

Acknowledgements

The authors gratefully acknowledge the Penn Institute for Regenerative Medicine, and funding from the David and Lucile Packard Foundation (JAB) and the National Science Foundation Graduate Research Fellowship Program (SK, JSK).

References

- 1 B. Gumbiner, *Cell*, 1996, **84**, 345–357.
- 2 J. Moon, M. Hahn, I. Kim, B. Nsiah and J. West, *Tissue Eng., Part A*, 2008.
- 3 C. Salinas and K. Anseth, *J. Tissue Eng. Regen. Med.*, 2008, **2**, 296–304.
- 4 L. Santiago, R. Nowak, J. Peter Rubin and K. Marra, *Biomaterials*, 2006, **27**, 2962–2969.
- 5 Z. Zhang, S. Chen and S. Jiang, *Biomacromolecules*, 2006, **7**, 3311–3315.
- 6 H. Senechal, J. Wahrman, D. Delain and M.-C. A, *In Vitro*, 1984, **20**, 692–698.
- 7 F. Scintu, C. Reali, R. Pillai, M. Badiali, M. Sanna, F. Argioli, M. Ristaldi and V. Sogos, *BMC Neurosci.*, 2006, **7**, 14.
- 8 F. Watt, *J. Cell Sci. Suppl.*, 1987, **8**, 313–326.
- 9 N. Ogura, M. Kawada, W. Chang, Q. Zhang, S. Lee, T. Kondoh and Y. Abiko, *J. Oral Sci.*, 2004, **46**, 207–213.
- 10 R. Salasnyk, W. Williams, A. Boskey, A. Batorsky and G. Plopper, *J. Biomed. Biotechnol.*, 2004, **2004**, 24–34.
- 11 Y. M. Shin, K.-S. Kim, Y. M. Lim, Y. C. Nho and H. Shin, *Biomacromolecules*, 2008, **9**, 1772–1781.
- 12 J. Curran, R. Chen and J. Hunt, *Biomaterials*, 2005, **26**, 7057–7067.
- 13 J. Curran, R. Chen and J. Hunt, *Biomaterials*, 2006, **27**, 4783–4793.
- 14 F. Watt, P. Jordan and C. O'Neill, *Proc. Natl. Acad. Sci. U. S. A.*, 1988, **85**, 5576–5580.
- 15 M. Lutolf, G. Raeber, A. Zisch, N. Tirelli and J. Hubbell, *Adv. Mater.*, 2003, **15**, 888–892.
- 16 T. Kraehenbuehl, P. Zammaretti, A. Van der Vlies, R. Schoenmakers, M. Lutolf, M. Jaconi and J. Hubbell, *Biomaterials*, 2008, **29**, 2757–2766.
- 17 J. Kim, Y. Park, G. Tae, K. Lee, S. Hwang, I. Kim, I. Noh and K. Sun, *J. Mater. Sci., Mater. Med.*, 2008, **19**, 3311–3318.
- 18 A. Gobin and J. West, *FASEB J.*, 2002, **16**, 751–753.
- 19 B. Mann, A. Gobin, A. Tsai, R. Schmedlen and J. West, *Biomaterials*, 2001, **22**, 3045–3051.
- 20 K. Nguyen and J. West, *Biomaterials*, 2002, **23**, 4307–4314.
- 21 Y. Luo and M. Shoichet, *Nat. Mater.*, 2004, **3**, 249–253.
- 22 P. Musoke-Zawedde and M. Shoichet, *Biomed. Mater.*, 2006, **1**, 162–169.
- 23 C. Chung, J. Mesa, M. Randolph, M. Yaremchuk and J. Burdick, *J. Biomed. Mater. Res. A*, 2006, **77**, 518–525.
- 24 C. Williams, A. Malik, T. Kim, P. Manson and J. Elisseeff, *Biomaterials*, 2005, **26**, 1211–1218.
- 25 J. Leach, K. Bivens, C. Collins and C. Schmidt, *J. Biomed. Mater. Res. A*, 2004, **70**, 74–82.
- 26 T. Bitter and H. Muir, *Anal. Biochem.*, 1962, **4**, 330–334.
- 27 D. Jiang, J. Liang and P. Noble, *Annu. Rev. Cell Dev. Biol.*, 2007, **23**, 435–461.
- 28 S. Yung, G. Thomas and M. Davies, *Kidney Int.*, 2000, **58**, 1953–1962.
- 29 J. Baier Leach, K. Bivens, C. J. Patrick and C. Schmidt, *Biotechnol. Bioeng.*, 2003, **82**, 578–589.
- 30 C. Chung, J. Mesa, G. Miller, M. Randolph, T. Gill and J. Burdick, *Tissue Eng.*, 2006, **12**, 2665–2773.
- 31 Y. Sakai, Y. Matsuyama, K. Takahashi, T. Sato, T. Hattori, S. Nakashima and N. Ishiguro, *Biomed. Mater. Eng.*, 2007, **17**, 191–197.
- 32 S. Sahoo, C. Chung, S. Khetan and J. Burdick, *Biomacromolecules*, 2008, **9**, 1088–1092.
- 33 Y. Ji, K. Ghosh, X. Shu, B. Li, J. Sokolov, G. Prestwich, R. Clark and M. Rafailovich, *Biomaterials*, 2006, **27**, 3782–3792.
- 34 M. Carroll, J. Cheeseman, R. Osman and H. Weinstein, *J. Phys. Chem.*, 1989, **93**.
- 35 M. Gibas and A. Korytkowska-Walach, *Polym. Bull.*, 2003, **51**, 17–22.
- 36 M. Hahn, L. Taite, J. Moon, M. Rowland, K. Ruffino and J. West, *Biomaterials*, 2006, **27**, 2519–2524.
- 37 S. Lee, J. Moon and J. West, *Biomaterials*, 2008, **29**, 2962–2968.